Journal Pre-proof

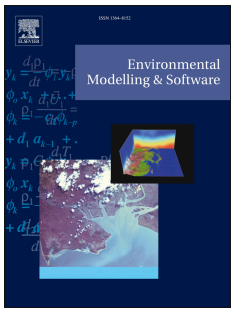

Vulnerability assessment of drinking water supply under climate uncertainty using a river contamination risk (RANK) model

Faranak Behzadi, Asphota Wasti, Todd E. Steissberg, Patrick A. Ray

PII: S1364-8152(21)00336-4

DOI: https://doi.org/10.1016/j.envsoft.2021.105294

Reference: ENSO 105294

To appear in: *Environmental Modelling and Software*

Received Date: 4 March 2021

Revised Date: 5 December 2021

Accepted Date: 23 December 2021

Please cite this article as: Behzadi, F., Wasti, A., Steissberg, T.E., Ray, P.A., Vulnerability assessment of drinking water supply under climate uncertainty using a river contamination risk (RANK) model, *Environmental Modelling and Software* (2022), doi: https://doi.org/10.1016/j.envsoft.2021.105294.

Vulnerability assessment of drinking water supply under climate uncertainty using a river contamination risk (RANK) model

Faranak Behzadi[1*], Asphota Wasti[1*], Todd E. Steissberg[3*], Patrick A. Ray[1*]

[1] *Environmental Engineering Department, University of Cincinnati, Cincinnati, OH, USA*

[3] *U.S. Army Engineer Research and Development Center*

Abstract

A river contamination risk (RANK) framework is developed to demonstrate the application of a Computational Fluid Dynamics model in risk assessment of contamination exposure in surface waters. The ultimate goal is to identify the factors responsible for potential future river contamination emergencies, and the use of that insight to inform strategic investments in resilience-enhancing infrastructure and policies. The RANK model is applied to preliminary assessment of a historical contamination event in the Ohio River. The results prove that with higher river velocity, plume passage becomes faster, with earlier peak time and shorter duration of plume at the point-of-interest. For the case under study, with increasing the initial spill duration by 100%, the plume duration at the point-of-interest may increase 85% or 65% depending on the toxicity level of the contaminant. The sensitivity analysis on hydraulic inputs implies that RANK can be utilized for climate-informed decision analysis in water quality applications.

Keywords: River water quality, Chemical spills, Computational Fluid Dynamics, Risk assessment, Ohio River

*Corresponding author

Email address: faranakb62@gmail.com (Faranak Behzadi[1])

1. Introduction

Approximately 50% of the world's people live within 3 km of a river [1], and are vulnerable to streamflow extremes (flood/drought) and poor water quality. These two problems are linked (and likely to worsen with climate change [2, 3]); however, the impact of streamflow extremes on water quality has not been given adequate attention in the scientific literature to date [4]. Floods mobilize contaminants stored on the floodplain [5] and overwhelm containment and treatment works. Droughts lower water levels, elevating pollutant concentrations, and stagnating flows (decreasing river re-oxygenation). In combination with warming waters, droughts increase the likelihood and severity of harmful algal blooms (HABs) [6].

Among its many current effects on the United States, climate change is raising mean temperature and increasing heavy precipitation events [7]. These changes, in combination with evolving flow regulation strategies and watershed development, are magnifying floods throughout the United States [8] and Europe [9], and likely elsewhere [10, 11, 12]. Droughts, on the other hand, concentrate contaminants, desiccate crops, and increase competition for water. Projections for mid-century indicate a high likelihood of increased precipitation extremes [13], with shifting seasonality and reductions in winter snowpack [10] altering the timing and magnitude of peak streamflow outside of the design range of existing infrastructure and their operating rules. Therefore, in the process of reducing risks to riparian communities, the compounding effects of streamflow extremes on water quality require careful exploration. Most of the work done in risk management and adaptive capacity [14, 15] has focused on issues of "available water" [16, 17, 18] or flood risk [19, 20, 21, 22, 23] in isolation, with promising nascent work in tradeoffs between ecological water needs and anthropocentric water supply [24, 25, 26]. The state of the art in climate change risk management is less mature in other aspects of water-resource systems. Though much progress has been made, for example, in the fields of computational fluid dynamics (CFD) and water supply risk assessment (including climate change risk) independently, surprisingly little work has been done to combine the tools of bottom-up water-resource system risk assessment (e.g., weather generators, hydrologic models, demographic and land use models, economic trade-off analysis, Bayesian networks) and contaminant transport (advection, dispersion and reaction of contaminants in flowing water) [27, 28], as has been done in coupled human-hydrologic system modeling.

Several studies have investigated the effect of climate change on riverine water quality [29, 30, 31, 32, 33]. These studies mostly focused on questions of contaminant (or nutrient) loading, as opposed to transport, and give particular attention to temperature effects [34]. These studies examined the influence on water quality of changes to climatic variables by monitoring water quality parameters during a specific time period, but were not able to simulate the pollutant fate under changing climate. Other studies related to climate change impacts on water quality have mostly focused on non-point source pollution in agricultural watersheds [35, 36, 37, 38, 39]. Although a few studies [40, 41] have been conducted to assess the impacts of climate change on pollutant transport, they have not investigated the effect of climate change and extreme events on the fate of point sources contamination and chemical spills in rivers. As such, contaminant transport models have not been included in water system modeling chains, and water quality concerns have therefore not been directly incorporated into bottom-up assessments of broader water system resilience.

Previous approaches to risk assessment or uncertainty analysis in problems of surface water contaminant transport have been almost exclusively of the one-dimensional (1D) type [42, 43, 44, 45, 46, 47], and have not been able to adequately reproduce contaminant plume duration. Contaminant plume exposure is typically the issue of greatest concern to riparian water utilities, and the inability to accurately model it diminishes the usefulness of 1D water quality risk assessment tools. Higher-dimensional CFD models are powerful tools to simulate the advection and dispersion of pollutants in surface waters. Many researchers have employed numerical models to simulate riverine pollutant transport [48, 49, 50], but have done so without evaluation of water contamination model response to hydro-climatological inputs. Van Griensven and Meixner [28] found that the major uncertainty in contaminant transport models relates to the form of the model (i.e., how the processes are represented), which indicates the importance of the two-dimensional (2D) CFD formulation, and a well-parameterized coupled human-hydrologic model for generation of CFD inputs. Additionally, previous approaches to climate change risk assessment in contaminant transport problems have tended to evaluate uncertainty in single inputs (e.g., meteorological [27]), but a systematic exploration of a multidimensional risk space is needed [51, 52].

Risk assessment in contaminant transport using 2D or three-dimensional (3D) model formulations have predominated in applications relating to the subsurface [53], but do not have obvious carry-over to riverine problems. The

standard tools available for 2D or 3D contaminant transport in surface water, such as the USEPA's Water Quality Analysis Simulation Program (WASP) [54, 55] and Environmental Fluid Dynamics Code (EFDC) [56, 57], are not appropriate for use in a risk assessment framework. Though excellent for their purposes, they are complex, slow, and data-intensive. Furthermore, they do not easily support batch runs (batch runs allow multiple runs of a model with one model call). In contrast, risk assessment requires many simulations to explore a decision space. Hence, more parsimonious and customizable models than EFDC/WASP (or others like them) are needed for large watersheds. Innovation in contaminant transport modeling is required.

Much progress has been made in the simulation of riverine sediment transport, which is largely now conducted in 2D and 3D (e.g., [58, 59]). Specific achievements of the sediment modeling community include lock-and-dam sediment entrainment and release [60], estimation of bed erosion effects [61], and improvements in calculation speed [62]. These experiments in sediment transport tend to be conducted as historical retrospectives, as opposed to risk assessment exercises, with the exception of studies such as Taner et al. [63] and Wild and Loucks [64], that factor sediment accumulation into overall vulnerability assessments of reservoir performance. Lessons learned from their methods are applied to the risk assessment approach developed in this work.

In summary, the scarcity of studies including contaminant transport models in planning-oriented scenario-exploration modeling chains [65, 66] has three primary causes: 1) existing contaminant transport models have mostly been developed for simulation of singular historical events, and are ill-fit for inclusion in a risk assessment framework requiring exploration of many scenarios in which variable inputs and even endogenous model process parameters are uncertain; 2) most candidate contaminate transport models are of the 1D type, but 2D or 3D contaminant behavior is often needed for simulation accuracy; and 3) guidance for systematic evaluation of plausible variability in hydraulic and spill characteristics has not been available.

The present study demonstrates the ability of a generalizable 2D CFD model to provide insight into the risk of contamination plume exposure in excess of a threshold. The sensitivity analysis on the hydraulic inputs demonstrates the beginnings of a path forward for climate-informed decision analysis [65] in water quality applications. The ultimate aim is to identify the specific factors responsible for compound events of streamflow extremes (flood or drought) and river contamination events, and the use of that insight to

inform strategic, staged early planning in resilience-enhancing infrastructure and policies. This work provides an opportunity for utilities to plan for potential contamination emergencies associated with climate-change-induced variations in streamflow. Stress tests should be conducted for water utility systems not only for changes in water quantity, but also for the impact those water volume changes might have on riverine contamination. The present analytical process presents utilities with a pathway to identification of the conditions likely to result in water system failures due to river contamination, so that system vulnerabilities might be reduced. The research uses a case study of a 48-kilometer section of the Ohio River upstream of Cincinnati. The developed framework is applied to preliminary assessment of the risk of various Ohio River flow velocities and plume attributes on a historical water contamination event.

2. Methodology

2.1. Framework for Point-of-Interest (PI) risk assessment based on uncertainties

The river contamination risk (RANK) workflow is a chain of data, models and visualizations capable of identifying riverine water quality risks as functions of hydrological and contaminant characteristic indicators (Figure 1). Hydrodynamics and pollutant fate and transport components of RANK are configured using a CFD model developed by Behzadi et al. [66, 67], which routes both the water and contaminants downstream. The accuracy and robustness of the model was verified and validated in their work using various analytical and experimental cases. Digital Elevation Models (DEMs) are the sources of topographical information of the river of interest (geometry and bathymetry) and are used to generate the computational mesh as an input to the RANK model. The underlying distribution, which governs the historical river flow data, is identified through standard statistical procedures and is the first input of the CFD model. Contaminant characteristics (e.g., plume duration and peak concentration), are altered as direct input to the CFD model. Infrastructure operation policies as well as forecasted data can also be input to the RANK algorithm to explore and predict the current and future water quality risks. Post-processing visualizations illustrate pollutant spread with river flow. Breakthrough curves of pollutants at points-of-interest (PI, defined by the user) show the time of travel, duration, and peak concentration of the plume. These are the key parameters in health impact evaluations

[68]. Risk assessments and stress tests are conducted through running various scenarios of uncertain parameters and infrastructure management policies.

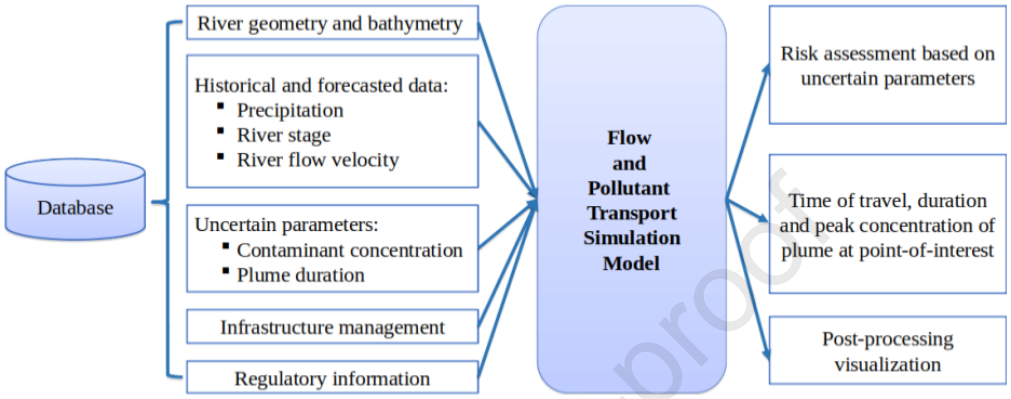

Figure 1: The river contamination risk (RANK) workflow for risk assessment of river pollution accidents at the point-of-interest (PI).

The RANK model aims to address the limitations of current water quality models by establishing a two-dimensional finite volume based model. Flow and transport equations are time-dependent and fully coupled to develop a robust and accurate model. The RANK model allows for real-world uncertainty including climate, land use, non-point source runoff risks, and human infrastructure operation. The following standard and widely-used water quality models are listed in Table 1 and compared to the present RANK model. 1) The Riverine Spill Modeling System (RSMS) was developed to predict the transport of a constituent as a result of a spill of known quantity and duration, at a known point on a river or first-order tributary of that river. The RSMS uses the one-dimensional Branched Lagrangian Transport Model (BLTM) and USACE CASCADE model to estimate the pollutant concentration and to predict plume time-of-travel, leading edge, peak, and trailing edge [69]. 2) The Hydrologic Engineering Center's River Analysis System (HEC-RAS) software, developed by the US Army Corps of Engineers (USACE), allows for one-dimensional sediment transport computations and water quality analyses [70]. 3) The Water Quality Analysis Simulation Program (WASP) is a dynamic fate and transport model, developed by US Environmental Protection Agency (USEPA), which simulates concentration of environmental contaminants in surface waters in one, two, or three dimensions. WASP should be linked with hydrodynamic models to provide flows, depths, and

velocities [71]. 4) The Environmental Fluid Dynamics Code (EFDC) is a surface water modeling system, developed by US Environmental Protection Agency (USEPA), which includes hydrodynamic and contaminant components [72] (see Table 1).

River water mixes with groundwater as it is diverted along subsurface flow paths, bringing with it a myriad of chemical solutes that are transported throughout the shallow streambed by advective and dispersive processes [73]. While the groundwater may affect the pollutant transport for low flow condition of the river, in the current study the focus is on the mass transport in surface waters and showing the accuracy and risk assessment capability of the RANK framework compared to widely-used water quality models.

2.2. Computational Fluid Dynamics (CFD) model

The three components of the applied computational algorithm are: mathematical modeling, grid generation, and numerical discretization. Each component is described in the following sections. The Riemann flux approximation [74] and a source-term balancing method [75, 76] is applied to develop a well-behaved and well-balanced numerical scheme.

Governing system of equations. The Shallow Water Equations (SWEs) are a set of nonlinear hyperbolic equations well established in water resources management to mathematically describe long wave hydrodynamics of free surface flows when the vertical acceleration of the water particles has a negligible effect on the pressure [77]. In this study the two-dimensional shallow water equations coupled with the depth-averaged scalar transport equation presented in [66] are applied in the computational algorithm to simulate the flow field and plume passage simultaneously. The non-dimensional form of the SWEs system may be written in conservative form as

$$\frac{\partial Q}{\partial t} + \frac{\partial F(Q)}{\partial x} + \frac{\partial G(Q)}{\partial y} + S(Q) = 0 \tag{1}$$

$$Q = \left\{ \begin{array}{c} h \\ h\,u \\ h\,v \end{array} \right\} \tag{2}$$

$$S = \left\{ \begin{array}{c} 0 \\ -(h-h_s)\frac{\partial h_s}{\partial x} + \tau_{bx} \\ -(h-h_s)\frac{\partial h_s}{\partial y} + \tau_{by} \end{array} \right\} \tag{3}$$

Table 1: Comparison of widely used water quality models with the present RANK model.

RANK	**RSMS [69]**
• 2D model capable of simulating both longitudinal and lateral dispersion of contaminant • capable of simulating both point and non-point source • capable of handling infrastructure operations • capable of run in a continuous period of time for large reaches	• 1D model incapable of simulating lateral flow and dispersion of contaminant • unable to handle non-point source pollution • unable to handle infrastructure operations • has to be run in discrete series of start/stop simulations • unable to handle a single run of the whole reach
RANK	**HEC-RAS [70]**
• flow and transport equations are 2D and capable of simulating both longitudinal and lateral dispersion of contaminant • capable of handling many simulations for use in a risk assessment framework	• 1D advection-dispersion equation for water quality simulation unable to reproduce lateral spreading of plume • currently not well suited for risk assessment framework
RANK	**WASP [71]**
• simulates both flow routing and contaminant transport simultaneously and in a time-dependent manner • capable of handling many simulations for use in a risk assessment framework	• has to be linked with a hydrodynamic model to calculate flowrate and velocity components and use them as inputs • not appropriate for use in a risk assessment framework, as doesn't support batch runs
RANK	**EFDC [72]**
• flow and transport equations are fully coupled and are solved simultaneously • supports unstructured meshes, allowing better representation of complex geometry, varied cell sizes, and rapid changes in cell sizes, improving accuracy and computational efficiency • finite volume model, improving mass conservation • suitable for risk assessment framework	• sequentially solves the external mode equations (depth integrated continuity and momentum equations), the internal mode equations (shear stresses), and the transport equations • often overparameterized and highly complex • slow and unequipped for uncertainty in many inputs • does not support unstructured meshes • finite difference model • not suitable for risk assessment framework

$$F = \begin{Bmatrix} h\,u \\ h\,u^2 + \frac{1}{2}(h^2 - h_s^2) \\ h\,u\,v \end{Bmatrix} \tag{4}$$

$$G = \begin{Bmatrix} h\,v \\ h\,u\,v \\ h\,v^2 + \frac{1}{2}(h^2 - h_s^2) \end{Bmatrix} \tag{5}$$

where h and h_s are the water depth and the bed level, respectively, and u and v are velocity components. τ_{bx} and τ_{by} denote frictional stresses on the

bottom, which are defined as (the Chezy model [78])

$$C = \frac{R^{1/6}}{n} \tag{6}$$

$$\tau_{bx} = \frac{g\,u\sqrt{u^2+v^2}}{C^2} \tag{7}$$

$$\tau_{by} = \frac{g\,v\sqrt{u^2+v^2}}{C^2} \tag{8}$$

Here C is the Chezy number, n is the Manning coefficient, R is the hydraulic radius approximated based on the flow depth h, and g is the gravitational acceleration constant.

Grid generation. In order to apply the conservation laws and implement the mathematical formulation, the pre-processing step in computational modeling is the discretization of the geometry of the river of interest into discrete volumes. A well-constructed mesh significantly improves the accuracy of the solution. In the present study, an unstructured mesh is generated to determine nodes and triangular elements connectivity. Unstructured meshes offer flexibility to conform to complex geometries, convenient refinement and de-refinement, and rapid change from small to large elements.

Numerical discretization. Among options for numerical scheme, finite volume methods have been extensively applied to simulate flow and mass transport, mainly due to the mass conservation property and lower memory requirements [79]. The finite volume method discretizes directly the integral form of equations (mass, momentum, and transport equations in the present study) over an arbitrary fixed domain. In this study, the spatial domain is divided into triangular cells, and a node-centered finite volume scheme is applied based on the median dual control volume. To evaluate a conservative and well-behaved flux at each control-volume interface, the primitive-variable Roe scheme is applied using the Roe-averaged values. Second-order accuracy is used in space and time with a nonlinear implicit scheme based on a Newton-iterative algorithm for the time integration. For an implicit scheme, the system of nonlinear equations must be linearized using a Newton-iterative algorithm [80], and the resulting sparse linear system is solved at each Newton iteration using the Gauss-Seidel stationary iterative method [81]. The

mathematical formulation and the source term balancing scheme utilized in this study satisfies still-water equilibrium on the arbitrary bed topography and allows for possible wet and dry interfaces within the solution domain, which are essential components in river flow simulations.

3. Ohio River basin case study

After the Mississippi River, the Ohio River is the largest by flow in the United States, and it suffers from contamination, low-water navigation restrictions, and flooding. The river supports centers of American agriculture, energy, and industry, transports approximately $40 billion worth of goods each year, and provides cooling or turbine water for approximately 450 power plants located within the watershed mainstem [82]. More than 27 million people live within the Ohio River watershed, 5 million of whom obtain their drinking water from the mainstem [82], and in 2016 it was described by the United States Environmental Protection Agency (USEPA) as the most contaminated surface water body in the United States [83]. The contaminants of greatest concern are nutrients and mercury [84], though the river also suffers from high levels of legacy organochlorines (e.g., PCBs), "emerging compounds" (e.g., PBDEs), and PFOA [85]. The people who obtain their drinking water directly from the Ohio River are subject to frequent contamination events. Ohio River flow velocity ranges more than an order of magnitude from approximately 0.09 to 3.2 m/s. Climate change effects such as increased evapotranspiration, seasonal precipitation shift and concentration of precipitation in already-wet months may change the factors dictating river flows and velocities in the future [86].

Water quality monitoring and modeling in the Ohio River basin is a collaborative effort, involving the National Weather Service (hydrologic modeling, stream routing and operational river forecasting [87]), the US Army Corps of Engineers (reservoir and infrastructure modeling), and the Ohio River Valley Water Sanitation Commission (contaminant transport modeling in cooperation with the US Geological Survey and the US Environmental Protection Agency). Local utilities, such as the Greater Cincinnati Water Works (GCWW), participate as well, and are stakeholders in the operation of a tool called the Ohio River Community Model [88]. The model is based on one-dimensional HEC-RAS routing, supplemented with a BLTM (see previous description of the RSMS model), requires disjoint, stitched model runs

at short time horizons, and performs poorly in the estimation of contaminant plume duration.

3.1. Case study of Cincinnati

GCWW, Cincinnati's public water supply utility, provides 416 million liters per day to approximately 1.1 million residents of southwest Ohio and northern Kentucky. Eighty percent of GCWW water supply is taken directly from the Ohio River [89], with the remaining twenty percent extracted from groundwater within the hydrologically-distinct Miami River basin 50-60 kilometers away. GCWW maintains offline storage equivalent to approximately 2 days of total demand, meaning that in an emergency it could close its Ohio River intake and draw from storage for up to approximately 48 hours. Three recent events have demonstrated the risks facing GCWW supply integrity, which represent the kinds of events that must be expected in the future, and against which the water system must be made resilient: 1) the Freedom Industries, West Virginia, 4-methylcyclohexane methanol (MCHM) spill of January 2014 [68]; 2) a diesel oil spill at a New Richmond, Ohio, Duke Energy generating facility in August 2014 [90]; and 3) the Southern Towing ammonium nitrate spill caused by a barge hull failure on the Benchmark River, Cincinnati, Ohio, in December 2017 [91]. Other spills occur with at least annual regularity, with evidence of linkages between historical flood events and microbial and chemical contamination of the river [92]. While none of these events resulted in water supply interruptions for Cincinnati, Cincinnati has on these and other occasions narrowly avoided disastrous water supply disruptions because of favorable hydrologic conditions. These conditions are subject to changing likelihoods in the future. It is reasonable to expect that water supply interruptions might have occurred, had hydrological and/or contaminant conditions been slightly different. Furthermore, Cincinnati's relative invulnerability may not apply to other cities drawing water from the Ohio River, with less offline storage or less robust water treatment infrastructure.

4. Model validation: Freedom Industries spill of 2014

On January 9, 2014, an estimated 37,854 liters of crude MCHM, an organic solvent used in coal processing, was released from a Freedom Industries facility into the Elk River, a tributary of the Kanawha River, near Charleston, West Virginia (Figure 2a). The chemical spill occurred just 1.61 kilometers

upstream from an intake to the Kanawha Valley Water Treatment Plant, which left almost 300,000 residents in nine West Virginia counties without access to potable water [45]. The developed RANK model is configured and applied for a 48-kilometers section of the Ohio River from Meldahl dam to Cincinnati including the GCWW water intake (Richard Miller Treatment Plant: RMTP). The goal is to simulate and reproduce the Freedom Industries spill of MCHM into the Ohio River in January 2014 and conduct a stress test on Cincinnati's drinking water vulnerability following the spill. DEMs are used to extract the geometry and bathymetry of the river portion of interest, which are later employed to generate the computational mesh. The required data (e.g. River velocity at Meldahl, MCHM measurements at Meldahl, Beckjord, and RMTP, river stage and discharge per availability) were collected from U.S. Geological Survey (USGS) website [93] and the Water Quality and Treatment Division of GCWW.

Figure 2b presents the geometry and the computational grid for the portion of the Ohio River under study. The two-dimensional unstructured mesh is generated once before starting the CFD simulation. For the current study, a uniform mesh is preferred to obtain the same accuracy throughout the domain. However, if a higher solution accuracy is required at the point-of-interest, the mesh may be refined near its location. The average grid spacing of the computational domain is 40 (m), resulting in 31,015 computational grid cells and the average total CPU time for simulation runs is approximately 24 hours (CPU with Turbo: Intel Xeon E5-2637 v4 (16) @ 3.700GHz).

A no-slip condition is enforced at side boundaries. An inlet boundary condition is imposed at the location of Meldahl Dam and a free outlet boundary condition is imposed at the Cincinnati location. The Gaussian function [94] is used to estimate the temporal distribution of measured MCHM level at Meldahl. The shape of the Gaussian function is determined by two parameters, mean (μ) and standard deviation (σ); thus, the initial concentration at Meldahl can be estimated as

$$\phi(t) = \frac{\alpha}{\sigma\sqrt{2\pi}} e^{\frac{-(t-\mu)^2}{2\sigma^2}} \tag{9}$$

where ϕ is the MCHM concentration (ppb: parts per billion), t is time in hours since time zero (in this case, hours after the Elk River spill started in Charleston, West Virginia), $\alpha = 220$, $\mu = 139.5$ and $\sigma = 4.5$. Model settings and parameters are summarized in Table (2).

The initial condition applied at Meldahl and the simulated breakthrough

Table 2: Numerical model settings and parameters for the case study of Ohio River reach from Meldahl to Cincinnati.

Model setup and parameters	Value
Initial river stage	12.2 (m)
Initial river flow velocity	1.6 (m/s)
Temporal distribution of MCHM concentration at Meldahl	Estimated by Equation (9)
Coefficient of MCHM distribution (α)	220
Mean of MCHM distribution (μ)	139.5
Standard deviation of MCHM distribution (σ)	4.5
Boundary	**Condition applied at the boundary**
Inlet (Meldahl)	Constant velocity of 1.6 (m/s)
Outlet (Cincinnati)	Free outflow
River sides	No-slip walls

curves at Beckjord and RMTP are visually compared to the sample data in Figure 3. Figure 4 displays three snapshots of the simulated contaminant dispersion in the Ohio River from Meldahl to Cincinnati. It shows that the plume arrives at Beckjord, and later at RMTP, after 135 hours and 140 hours, respectively. Plume arrival is calculated with the threshold of 1 ppb of MCHM concentration.

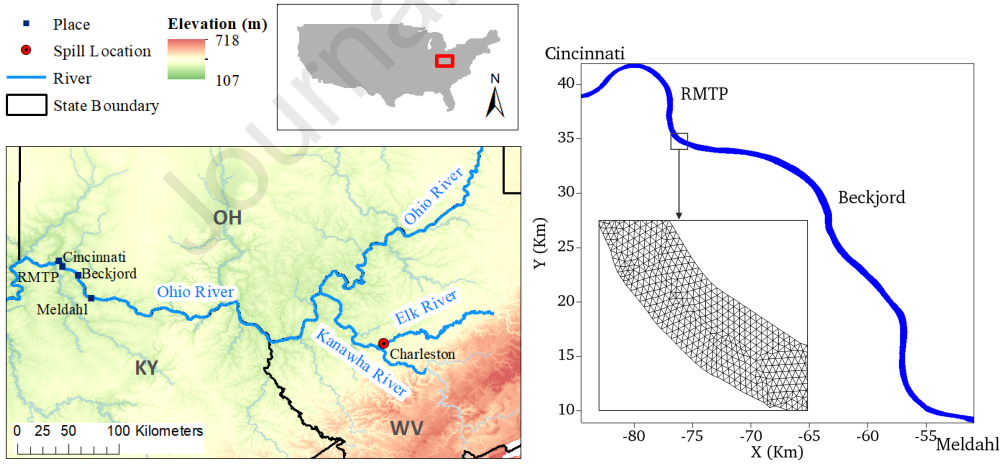

(a) (b)

Figure 2: a) Freedom Industries spill location, b) The portion of the Ohio River under study stretching from Meldahl dam to Cincinnati and the generated unstructured mesh.

Previous studies of this spill have presented one-dimensional models of flow and contaminant transport [45, 95]. These one-dimensional models do

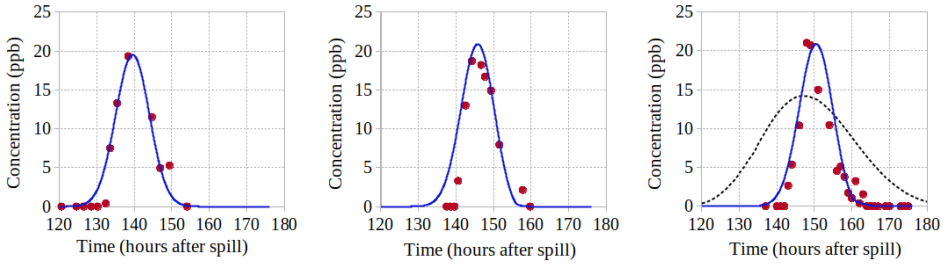

(a) Meldahl (b) Beckjord (c) RMTP

Figure 3: MCHM concentration of January 2014 Freedom Industries spill into the Ohio River. Solid line: RANK simulation results; Dots: sample data; Dashed line: the previous study of Bahadur and Samuels [45]. a) The initial condition estimated by Equation (9); b) simulated results at Beckjord compared with sample data; c) simulated results at RMTP compared with sample data.

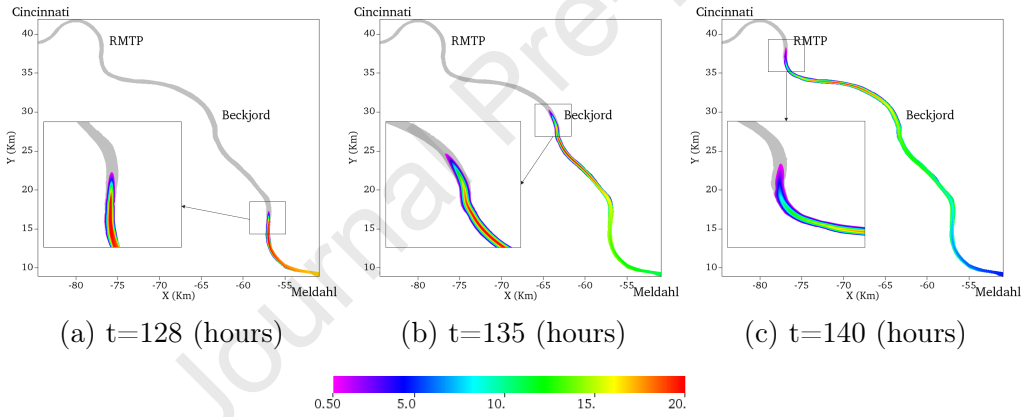

(a) t=128 (hours) (b) t=135 (hours) (c) t=140 (hours)

(d) Concentration (ppb)

Figure 4: Simulation results for contaminant dispersion in the Ohio River from Meldahl to Cincinnati (hours after the Elk River spill started in Charleston, West Virginia)

not consider the width and stage variations along the river reach [96], which limits their application to reaches with constant width and steady water depth. Moreover, the model in [45] is designed to evaluate the contaminant concentration only, without simulating the river hydrodynamics such as transient water stage and directional velocities. It uses mean flows and velocities from the existing datasets and updates these flows and velocities based on nearby real-time gauge readings. Whereas, the present RANK model prototyped in Figure 2 is two-dimensional, and capable of simulating longitudinal

and transverse velocity components based on variable time of arrival, time of peak, and duration of the plume at a PI as governed by the transient CFD equations. Figure 3c is a demonstration of improvements achieved on previous estimation of contaminant transport reproduction at the GCWW intake.

To quantify the agreement between the present model and the observations [97], plume passage characteristics evaluated at each location are presented in Table 3, and the related percent errors are compared in Table 4. The RANK model estimates the time of peak concentration with errors less than 2.3% at all three locations. According to the aforementioned differences in applying the velocity field, the error in peak concentration at RMTP is 32% in [45], while it is estimated with 0.95% error using the RANK model. It is reasonable to assume, based on visual inspection of the measured samples at Beckjord in Figure 3b, that the peak concentration may have occurred between two sampling moments, and thus the real peak was missed. This assumption would lead to the reported error at Beckjord calculated in Table 4 being interpretable as an overestimate. The duration of plume is reproduced using RANK at Beckjord and RMTP locations with 6.5% and 1.8% errors, respectively, while [45] shows 152% error in reproduction of the plume duration at RMTP.

Table 3: Comparison of plume passage characteristics and the percentage of errors (E), shown in Figure 3.

	Time of peak (hours after spill)			Peak concentration (ppb) [1]			Plume duration [2] (hours)		
Location	Meldahl	Beckjord	RMTP	Meldahl	Beckjord	RMTP	Meldahl	Beckjord	RMTP
Samples	138.4	144.25	148	19.3	18.7	21	24	20	22
RANK	139	145.8	151.4	19.5	20.9	20.8	22.4	21.4	22.4
[45] [3]	-	-	146.8	-	-	14.2	-	-	55.5

[1] parts per billion

[2] The plume duration is calculated with the threshold of 1 ppb of MCHM concentration.

[3] Bahadur and Samuels [45]

Table 4: The percentage of error in plume passage characteristics compared to sample data.

	Error in time of peak (%)			Error in peak concentration (%)			Error in plume duration (%)		
Location	Meldahl	Beckjord	RMTP	Meldahl	Beckjord	RMTP	Meldahl	Beckjord	RMTP
RANK	0.43	1.07	2.3	1.04	12	0.95	6.7	6.5	1.8
[45]	-	-	0.81	-	-	32	-	-	152

5. Risk assessment

For water quality risk assessment, a stress test can usefully be conducted on key factors of a contamination event, such as flow characteristics and spill duration. In this section, several scenarios of flow and contaminant characteristics are applied in the simulation of the MCHM spill in January 2014, and the results of the stress test are interpreted for their impact on Cincinnati's drinking water intake.

5.1. Flow characteristics

One of the principal drivers of pollutant transport in rivers is the flow velocity [98]. The annual maximum and minimum stages were obtained from the National Weather Service [99]. The annual peak discharge was obtained from HEC-SSP (HEC-Statistical Software Package), which automatically downloads the data from the USGS website. For the river portion shown in Figure 2, the historical stream velocity data is available for USGS station 03255000 located at Cincinnati, OH. A stage-discharge-velocity relationship is established with the data retrieved from [93] and the annual maximum velocities and annual minimum stages are presented in Figure 5. Given that the flow velocity during the historical event in January 2014 was not the peak for that year (see Figure 5a) and the maximum annual velocity in many other historical years was higher than 2014 (e.g., the largest flood in the history of Cincinnati occurred in January 1937), the flow velocity in January 2014 could have been much larger, with consequences to contaminant transport.

Unlike for high-velocity conditions, the historical record is a less useful reference for low-velocity conditions of the Ohio River. According to the Ohio River Valley Water Sanitation Commission (ORSANCO), there are twenty-one locks and dams constructed on the Ohio River, mostly after 1959 [100]. Locks and dams raise minimum stages during the low-flow period at the end of each summer (see Figure 5b), and slow river velocities, sometimes to near stagnation. This is of great benefit to navigation during summer and fall, but makes translation of river stage measurements into velocity values during dry periods nearly impossible.

To investigate the impact of flow velocities that can reasonably be expected to occur along this reach of the Ohio River, three low flow scenarios as well as three historical floods of Cincinnati, presented in Table 5, are selected for the stress test. These specific flows were chosen to include a broad

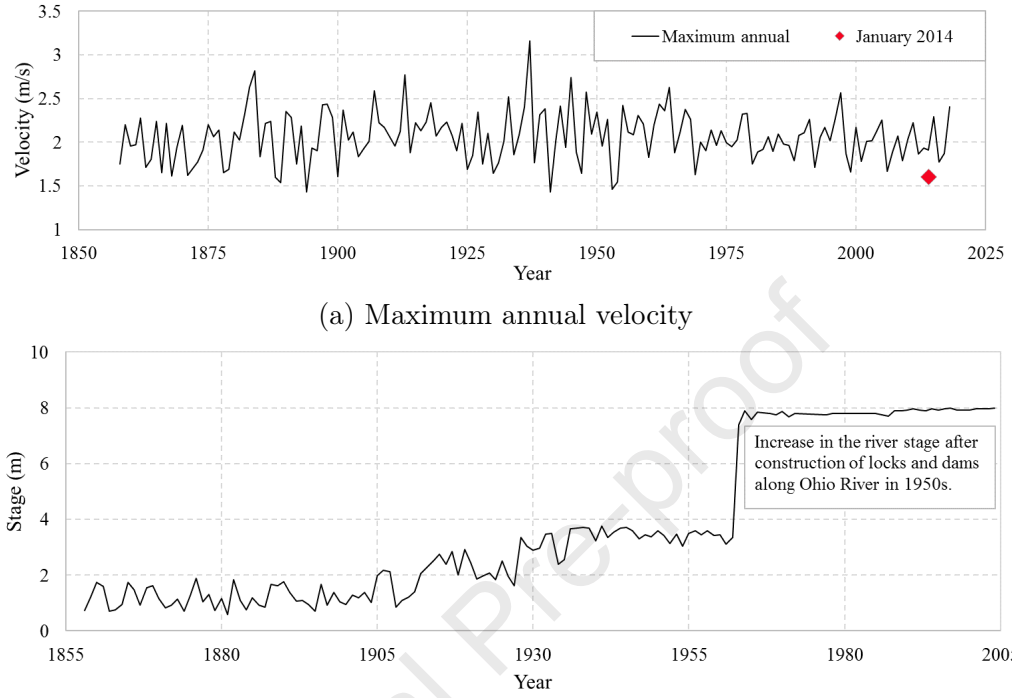

(a) Maximum annual velocity

(b) Minimum annual stage

Figure 5: Extreme annual river stage and velocity of the Ohio River at Cincinnati station (USGS 03255000). a) Maximum annual velocity. The river velocity during MCHM spill of 2014 is also shown for the sake of comparison. b) Minimum annual stage. Construction of locks and dams on the river increased the river stage in two phases, after 1921 and after 1959 [100].

range of velocity magnitude, severity level, and probability-of-exceedance. The research question is: What would happen to contaminant plume duration at the GCWW intake if the January 2014 MCHM spill had occurred instead during a low flow or high flow period, such as the July 1914 and March 1997 periods?

Low-velocity values were sampled from pre-1960 records, before the impacts of locks and dams on the Ohio River became dominant. During hot dry summers, such as occurred in the Ohio River basin in 2015, river velocities could decrease below the 0.31 m/s year 1914 minimum value used for this study, and exploration of the impact of lock and dam operation on contaminant plume passage is therefore an important subject for future study,

Table 5: Historical floods and low flows in Cincinnati used in the RANK model. These specific flows are chosen to cover a broad range of severity level for floods as well as historical low flows to cover the real flow range of the Ohio River.

Date	Flow (m^3/s)	Stage (m)	Velocity (m/s)
Jul 1914	506.87	1.37	0.31
Sep 1910	877.82	2.69	0.64
Jul 1955	1716.00	4.26	0.94
Jan 2014 *	8017.09	12.2	1.60
Jan 1951	11100.71	14.9	1.95
Jan 2005	14041.96	17.3	2.25
Mar 1997	17405.26	19.7	2.57

* Baseline.

beyond the scope of the current work. The highlighted row of Table 5 shows the velocity during the historical MCHM spill of January 2014.

5.2. Contaminant characteristics

Spill characteristics also indicate variations in the level of risk at the point-of-interest. Particularly for chemical spills upstream of water treatment plants, plume duration influences the time period during which the treatment plant should be shut down. This may result in drinking water shortage to the affected residents. Therefore, to evaluate the potential influences of spill perturbations on water supply interruption, the initial plume duration of spill 2014 (τ) at Meldahl is increased by 50% (1.5τ) and 100% (2τ).

5.3. Bathymetry

Another factor, which may impact the risk level at the point-of-interest, is the bathymetry of the river, i.e. the river bed topology. To evaluate the sensitivity of the drinking water supply to the bathymetry, the 2014 spill is reproduced with the actual and flat bed topology and the results are compared in the following section.

6. Results and Discussion

6.1. Flow and contaminant stress test

The selected flow characteristics (Table 5) combined with the plume characteristics of actual and extended MCHM spill of 2014 (Figure 6) were input

into the RANK model, and the output results are presented in Table 6 and Figure 7. Plume duration is evaluated at two threshold levels of contaminant concentration, 0.01 ppb and 1 ppb. The concentration of 1 ppb is selected because it represents the average detectable level of MCHM concentration according to sampling results [97] and West Virginia Testing Assessment Project (WV TAP) [101]. The concentration of 0.01 ppb is chosen solely for the purpose of risk assessment, to show that the toxicity threshold and detectable level of contaminant could also influence spill response strategies.

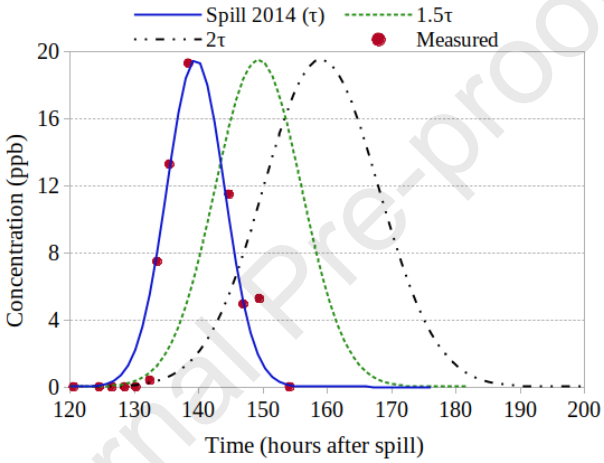

Figure 6: The initial plume duration at Meldahl (τ) is perturbed with 50% (1.5τ) and 100% (2τ).

Table 6: Stress test on river flow and plume characteristics at RMTP. The flow of spill 2014 replaced by historical floods and low flows of Cincinnati. The plume duration of spill 2014 at Meldahl (τ) is extended by 50% (1.5τ) and 100%(2τ).

		Time to Peak (hours after spill)			Plume duration (hours) safety level of 0.01 (ppb)			Plume duration (hours) safety level of 1 (ppb)		
Flow \ Plume	Velocity (m/s)	τ	1.5τ	2τ	τ	1.5τ	2τ	τ	1.5τ	2τ
Low flow 1914	0.31	258	268	278.2	93.1	103.2	114.4	40.4	50.5	61.7
Low flow 1910	0.64	179.5	189.5	199.7	83.2	96.7	110.5	28	38	46
Low flow 1955	0.94	162.6	172.7	182.8	72	85	104	25	32.5	41.5
Jan 2014	1.60	151.4	160.4	170.5	43.8	60.6	72.9	22.4	30.3	41.5
Flood 1951	1.95	148	158	167	34.8	49	64.8	20.2	30.3	42.3
Flood 2005	2.25	147	157	166	33.5	48	63.9	20.2	31.4	42.6
Flood 1997	2.57	145	156	165	32.4	47.1	63.4	20.2	31.4	42.6

The stress test results demonstrate that with higher river velocity, plume passage becomes faster, with earlier peak concentration time and shorter duration of plume at RMTP (Table 6). For instance, when the river velocity is increased by 60% (from January 2014 with velocity of 1.6 m/s to the flood of 1997 with velocity of 2.57 m/s), the plume arrives at its peak level at the RMTP location 6.4 hours earlier.When the river velocity is decreased by 81% (from January 2014 with velocity of 1.6 m/s to the flow of 1914 with velocity of 0.31 m/s), the time to peak concentration is delayed by 106.6 hours. These calculations presume a free-flowing, if slow, river. Note that the ability of locks and dams to retain river flows during dry periods, retarding river flow to the point of stagnation, has potential to fundamentally alter these calculations, and must be included in future, improved versions of contaminant transport hydraulic modeling.

Moreover, with the flow of January 2014, and increasing the initial spill duration by 100%, the plume duration at RMTP may increase 85% or 65% depending on the toxicity level of the contaminant.

Though the higher velocity results in a shorter shut-down period for the treatment plant, it leaves the water utility managers with less time to make an initial assessment of the spill and to decide on the emergency response. On the other hand, lower flow velocity imposes a higher risk on drinking water supply due to the longer period of the plant shut-down and limited off-line storage of drinking water.

The simulation results shown in Figure 7 indicate that lower river velocity and prolonged initial spill duration impose higher risks on the drinking water supply. If contaminant plumes at levels greater than human-health standards persist for more than two days, GCWW's offline storage is exhausted and municipal water supply interruptions to Cincinnati are likely to result. In particular, if the toxicity level of spilled chemical is determined at 0.01 ppb (Figures 7a and 7c), the drinking water storage is more at risk than at the toxicity level of 1 ppb (Figures 7b and 7d).

Figures 7c and 7d demonstrate the combination of river/contaminant conditions with two toxicity levels that may create failure at Cincinnati. Risks to water supply in Cincinnati are presented relative to critical threshold of plume passage duration (two days) at RMTP as a function of the initial spill duration at Meldahl and the river velocity. In the solid region of the plot the off-line storage is sufficient to cover a shutdown of the Ohio River intake until the plume passes the water intake; whereas the hatched zone indicates conditions leading to potential water supply disruptions. If the upstream

(Meldahl) contaminant plume passage lasted longer than 1.5τ and the river velocity were lower than 1.6 m/s, for example, then a failure would occur (at the threshold level of 0.01 ppb).

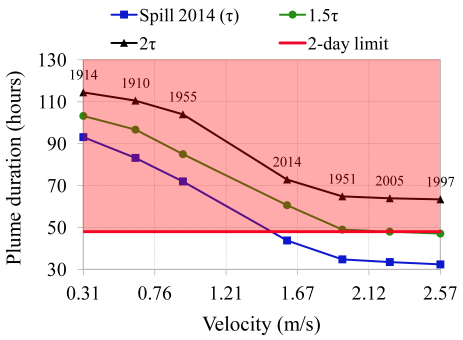

(a) Calculated plume duration at RMTP with safety level of 0.01 ppb.

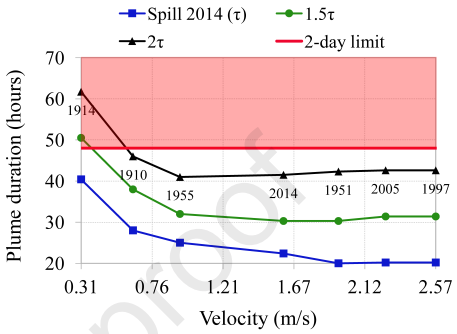

(b) Calculated plume duration at RMTP with safety level of 1 ppb.

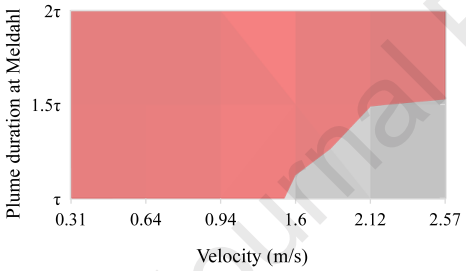

(c) Stress surface with safety level of 0.01 ppb.

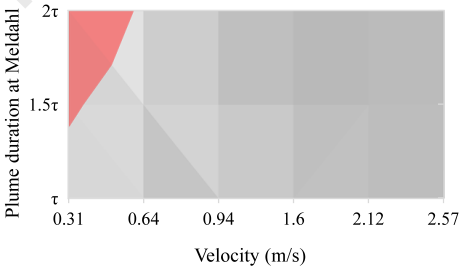

(d) Stress surface with safety level of 1 ppb.

Figure 7: Stress test on the MCHM spill of 2014 using historical floods and low flows presented in Table 5. The simulated plume duration at RMTP is compared for different initial spill duration (presented in Figure 6), with the safety level of (a) 0.01 ppb, and (b) 1 ppb. The labels show the year of the applied flow characteristics. Also, the stress surface on the duration of MCHM at RMTP with 48 hours storage capacity depicted at safety level of (c) 0.01 ppb, and (d) 1 ppb. For all subplots, the red zone presents the failure zone where the plume duration lasts more than two-day (48 hours) threshold of the off-line storage for Cincinnati's drinking water supply.

6.2. Bathymetry stress test

The previous simulations were carried out with the real bathymetry of the river. In this section, the sensitivity of the drinking water supply to the

river bathymetry is evaluated by comparing the RANK results for the real bathymetry and a uniform flat river bed. The flow and plume characteristics of MCHM spill of 2014 were input to the RANK model and the results are presented in Table 7. With a flat river bed, MCHM reaches its peak concentration at RMTP location approximately 8 hours earlier compared to the case with the real bathymetry. Lower plume duration is also detected in the case with a flat topography. These results confirm that the accuracy of the model in reproducing spill cases is crucial in assessing the risk of water supply interruption as the plume peak time and duration are the key factors in the water intake shutdown in case of a chemical spill.

Table 7: Bathymetry effect on plume characteristics at RMTP. The spill of January 2014 reproduced with the real bathymetry and the flat bed.

	Time to Peak (hours after spill)		Plume duration (hours) safety level of 0.01 (ppb)		Plume duration (hours) safety level of 1 (ppb)	
Flow and Plume conditions	Real Bathymetry	Flat bed	Real Bathymetry	Flat bed	Real Bathymetry	Flat bed
Jan 2014	151.4	143.14	43.8	39.96	22.4	21.03

7. Conclusion

This study demonstrated an application of a fluid dynamic model, RANK, to water quality risk assessment and its ability in evaluating risks of hydrologic/hydraulic change. The contribution of the developed model is twofold: 1) It allows for variable channel width, water depth, and velocity, which makes it more accurate and flexible than existing tools in application to complex study areas. The accuracy of the RANK model in reproduction of contaminant plume duration makes the water quality stress test possible. 2) It can be used for scenario analysis and stress testing by changing uncertain inputs as initial and boundary conditions, including flow velocity, non-point source pollution, infrastructure operating rules, biological activity (e.g., harmful algal blooms), and temperature effects. The model is also capable of applying time dependent velocity variations at every grid cell to address floods and runoff points. The RANK model is expected to be useful in a wide range of climate change risk assessments to evaluate the water quality impacts of flood and low flow. The sensitivity analysis on hydraulic inputs implies that the model can be utilized for climate-informed decision analysis [102, 65] in water quality applications. An initial prototype application of the

developed framework was presented in this paper and applied for evaluating the risks of water supply disruption in Cincinnati due to a historical chemical spill on the Ohio River. The next step in advancing RANK is to automate the process of the computational mesh generation based on existing Digital Elevation Models for the river of interest. Future research will use the RANK model to evaluate risks to water quality for riparian cities from potential future changes in climate, land use, and infrastructure operation. This will be accomplished by linking RANK into a workflow of simulation models including a weather generator (preferably one with direct linkages to physical climate processes, such as Steinschneider et al. [103]), a hydrologic model, and a reservoir operation model. This chain of models will allow careful attention to harmful algal blooms, and better understanding of the relative impacts of navigational, agricultural, and industrial sector impacts on water quality. Evaluation of the ecological responses to the river pollution could be another extension of the RANK model for future studies. In addition, future research should consider: 1) the groundwater contribution in driving the pollutant transport; and 2) a potentially evolving bathymetry. At its present execution speed, the RANK model is not easy to apply to long rivers, or to many simulations. The present study applies RANK to a 48-kilometers river reach, and to a handful of scenarios of possible future conditions. The aim for future applications is to apply RANK for long rivers under all scenarios resulting from full factorial combinations of many climate-related and non-climate uncertainties that may affect river contamination. For that purpose, RANK needs to respond faster by involving multiple computational cores which could be done through updating the existing model using parallel programming. At sufficiently fast computational speeds, the RANK tool might also be suitable for real-time operations and disaster response, but that purpose is beyond the current scope of study.

This study has taken a basic approach to climate change stress testing in the interest of demonstrating a proof-of-concept. The impact on water quality at the location of a riverine water intake was explored from delta-shifts in long-term average precipitation and temperature. The magnitude and direction of these delta-shifts were informed by the full ensemble of the current generation of General Circulation Model (GCM) output produced by the Intergovernmental Panel on Climate Change (IPCC). The delta-shifts in long-term average conditions were applied to alter the relatively short-duration spill event evaluated in this case. As new generations of IPCC model output become available, the delta-shifts should be updated to accommodate

evolving understanding of climate change science. However, exploration of the climate change impacts (e.g., increased evapotranspiration, seasonal precipitation shift, exacerbation of precipitation extremes) on water quality was outside of the scope of the present study, but is recommended as a subject for future research. Such studies are accomplishable with the RANK model presented here.

Acknowledgements

This research was supported by the Ohio Water Resources Center, Ohio State University PTE Federal Award 8293 Subaward 60070994. The fund was awarded to the first (FB) and last (PAR) authors.

[1] M. Kummu, H. de Moel, P. J. Ward, O. Varis, How close do we live to water? a global analysis of population distance to freshwater bodies, PLOS ONE 6 (2011) 1–13. doi:10.1371/journal.pone.0020578.

[2] D. Schiedek, B. Sundelin, J. W. Readman, R. W. Macdonald, Interactions between climate change and contaminants, Marine Pollution Bulletin 54 (2007) 1845–1856. doi:10.1016/j.marpolbul.2007.09.020.

[3] T. Hrdinka, O. Novický, E. Hanslík, M. Rieder, Possible impacts of floods and droughts on water quality, Journal of Hydro-environment Research 6 (2012) 145–150. doi:10.1016/j.jher.2012.01.008, Special Issue on Ecohydraulics: Recent Research and Applications.

[4] S. J. Khan, D. Deere, F. D. Leusch, A. Humpage, M. Jenkins, D. Cunliffe, Extreme weather events: Should drinking water quality management systems adapt to changing risk profiles?, Water Research 85 (2015) 124–136. doi:10.1016/j.watres.2015.08.018.

[5] K. R. Ryberg, W. Lin, A. V. Vecchia, Impact of climate variability on runoff in the North-Central United States, Journal of Hydrologic Engineering 19 (2014) 148–158. doi:10.1061/(ASCE)HE.1943-5584.0000775.

[6] W. K. Dodds, W. W. Bouska, J. L. Eitzmann, T. J. Pilger, K. L. Pitts, A. J. Riley, J. T. Schloesser, D. J. Thornbrugh, Eutrophication of U.S. freshwaters: Analysis of potential economic damages, Environmental Science & Technology 43 (2009) 12–19. doi:10.1021/es801217q, pMID: 19209578.

[7] D. J. Wuebbles, D. W. Fahey, K. A. Hibbard, B. DeAngelo, S. Doherty, K. Hayhoe, R. Horton, J. P. Kossin, P. C. Taylor, A. M. Waple, C. P. Weaver, D. J. Dokken, B. C. Stewart, T. K. Maycock, Executive summary, U.S. Global Change Research Program, Washington, D.C., 2017, pp. 12–34. doi:10.7930/J0DJ5CTG.

[8] R. M. Vogel, C. Yaindl, M. Walter, Nonstationarity: Flood magnification and recurrence reduction factors in the United States, Journal of the American Water Resources Association 47 (2011) 464–474. doi:10.1111/j.1752-1688.2011.00541.x.

[9] E. Fischer, R. Knutti, Observed heavy precipitation increase confirms theory and early models., Nature Climate Change 6 (2016) 986–991. doi:10.1038/nclimate3110.

[10] IPCC: Climate Change 2013, The Physical Science Basis. Contribution of Working Group I to the Fifth Assessment Report of the Intergovernmental Panel on Climate Change, 2013.

[11] IPCC: Climate Change 2015, Climate Change 2014: Synthesis Report. Contribution of Working Groups I, II and III to the Fifth Assessment Report of the Intergovernmental Panel on Climate Change, 2015.

[12] F. Behzadi, A. Wasti, S. Haque Rahat, J. N. Tracy, P. A. Ray, Analysis of the climate change signal in Mexico City given disagreeing data sources and scattered projections, Journal of Hydrology: Regional Studies 27 (2020) 100662. doi:10.1016/j.ejrh.2019.100662.

[13] IPCC: Summary for Policymakers, Managing the Risks of Extreme Events and Disasters to Advance Climate Change Adaptation. A Special Report of Working Groups I and II of the Intergovernmental Panel on Climate Change, 2012.

[14] S. Hallegatte, Strategies to adapt to an uncertain climate change, Global Environmental Change 19 (2009) 240–247. doi:10.1016/j.gloenvcha.2008.12.003, Traditional Peoples and Climate Change.

[15] N. L. Engle, Adaptive capacity and its assessment, Global Environmental Change 21 (2011) 647–656. doi:10.1016/j.gloenvcha.2011.01.019, Special Issue on The Politics and Policy of Carbon Capture and Storage.

[16] N. L. Miller, K. E. Bashford, E. Strem, Potential impacts of climate change on California hydrology, JAWRA Journal of the American Water Resources Association 39 (2003) 771–784. doi:10.1111/j.1752-1688.2003.tb04404.x.

[17] A. H. Arthington, R. J. Naiman, M. E. McClain, C. Nilsson, Preserving the biodiversity and ecological services of rivers: new challenges and research opportunities, Freshwater Biology 55 (2010) 1–16. doi:10.1111/j.1365-2427.2009.02340.x.

[18] D. Lettenmaier, A. Wood, R. Palmer, Water resources implications of global warming: A U.S. regional perspective., Climatic Change 43 (1999) 537–579. doi:10.1023/A:1005448007910.

[19] H. C. Winsemius, L. P. H. Van Beek, B. Jongman, P. J. Ward, A. Bouwman, A framework for global river flood risk assessments, Hydrology and Earth System Sciences 17 (2013) 1871–1892. doi:10.5194/hess-17-1871-2013.

[20] H. Kreibich, P. Bubeck, M. Vliet, H. Moel, A review of damage-reducing measures to manage fluvial flood risks in a changing climate, Mitigation and Adaptation Strategies for Global Change 20 (2015) 967–989. doi:10.1007/s11027-014-9629-5.

[21] J. D. Salas, J. Obeysekera, R. M. Vogel, Techniques for assessing water infrastructure for nonstationary extreme events: a review, Hydrological Sciences Journal 63 (2018) 325–352. doi:10.1080/02626667.2018.1426858.

[22] M. Karamouz, S. Nazif, Reliability-based flood management in urban watersheds considering climate change impacts, Journal of Water Resources Planning and Management 139 (2013) 520–533. doi:10.1061/(ASCE)WR.1943-5452.0000345.

[23] Q. Zhou, P. Mikkelsen, K. Halsnæs, K. Arnbjerg-Nielsen, Framework for economic pluvial flood risk assessment considering climate change effects and adaptation benefits, Journal of Hydrology 414-415 (2012) 539 – 549. doi:10.1016/j.jhydrol.2011.11.031.

[24] N. L. Poff, C. M. Brown, T. E. Grantham, J. H. Matthews, M. A. Palmer, C. M. Spence, R. L. Wilby, M. Haasnoot, G. F. Mendoza, K. C. Dominique, A. Baeza, Sustainable water management under future uncertainty with eco-engineering decision scaling, Nature Climate Change 6 (2016) 25–34. doi:10.1038/nclimate2765.

[25] A. C. Horne, R. Nathan, N. L. Poff, N. R. Bond, J. A. Webb, J. Wang, A. John, Modeling Flow-Ecology Responses in the Anthropocene: Challenges for Sustainable Riverine Management, BioScience 69 (2019) 789–799. doi:10.1093/biosci/biz087.

[26] A. John, A. Horne, R. Nathan, M. Stewardson, J. A. Webb, J. Wang, N. L. Poff, Climate change and freshwater ecology: Hydrological and ecological methods of comparable complexity are needed to predict risk, WIREs Climate Change 12 (2021) e692. doi:https://doi.org/10.1002/wcc.692.

[27] W. M. Angevine, J. Brioude, S. McKeen, J. S. Holloway, Uncertainty in lagrangian pollutant transport simulations due to meteorological uncertainty from a mesoscale WRF ensemble, Geoscientific Model Development 7 (2014) 2817–2829. doi:10.5194/gmd-7-2817-2014.

[28] A. van Griensven, T. Meixner, Methods to quantify and identify the sources of uncertainty for river basin water quality models, Water Science and Technology 53 (2006) 51–59. doi:10.2166/wst.2006.007.

[29] S. Rostami, J. He, Q. Hassan, Riverine water quality response to precipitation and its change, Environments 5 (2018) 8. doi:10.3390/environments5010008.

[30] J. Tu, Combined impact of climate and land use changes on streamflow and water quality in Eastern Massachusetts, USA, Journal of Hydrology 379 (2009) 268–283. doi:10.1016/j.jhydrol.2009.10.009.

[31] P. Whitehead, R. Wilby, R. Battarbee, M. Kernan, A. Wade, A review of the potential impacts of climate change on surface water quality, Hydrological Sciences Journal-Journal Des Sciences Hydrologiques 54 (2009) 101–123. doi:10.1623/hysj.54.1.101.

[32] A. Tariq, R. J. Lempert, J. Riverson, M. Schwartz, N. Berg, A climate stress test of Los Angeles water quality plans, Climatic Change 144 (2017) 625–639. doi:10.1007/s10584-017-2062-5.

[33] X. Wang, Z. Li, M. Li, Impacts of climate change on stream flow and water quality in a drinking water source area, Northern China, Environmental Earth Sciences 77 (2018) 410. doi:10.1007/s12665-018-7581-5.

[34] M. Benitez-Gilabert, M. Alvarez-Cobelas, D. Angeler, Effects of climatic change on stream water quality in Spain, Climatic Change 103 (2010) 339–352. doi:10.1007/s10584-009-9778-9.

[35] H. Chang, B. Evans, D. Easterling, The effects of climate change on stream flow and nutrient loading, Journal of the American Water Resources Association 37 (2001) 985. doi:10.1111/j.1752-1688.2001.tb05526.x.

[36] Y. Panagopoulos, P. Gassman, R. Arritt, D. Herzmann, T. Campbell, A. Valcu, J. Arnold, Impacts of climate change on hydrology, water quality and crop productivity in the Ohio-Tennessee river basin, International Journal of Agricultural and Biological Engineering 8 (2015) 36–53. doi:10.3965/j.ijabe.20150803.1497.

[37] G. Parker, R. Droste, K. Kennedy, Modeling the effect of agricultural best management practices on water quality under various climatic scenarios, Journal of Environmental Engineering and Science 7 (2008) 19. doi:10.1139/S07-026.

[38] E. Struyf, S. Van Damme, P. Meire, Possible effects of climate change on estuarine nutrient fluxes: a case study in the highly nutrified Schelde estuary (Belgium, The Netherlands), Estuarine, Coastal and Shelf Science 60 (2004) 649 – 661. doi:10.1016/j.ecss.2004.03.004.

[39] L. Wu, T. Long, X. Liu, J. Guo, Impacts of climate and land-use changes on the migration of non-point source nitrogen and phosphorus during rainfall-runoff in the Jialing River Watershed, China, Journal of Hydrology 475 (2012) 26–41. doi:10.1016/j.jhydrol.2012.08.022.

[40] E. Marshall, T. Randhir, Effect of climate change on watershed system: A regional analysis, Climatic Change 89 (2008) 263–280. doi:10.1007/s10584-007-9389-2.

[41] T. Nordam, D. Dunnebier, C. Beegle-Krause, M. Reed, D. Slagstad, Impact of climate change and seasonal trends on the fate of arctic oil spills, Ambio 46 (2017) 442–452. doi:10.1007/s13280-017-0961-3.

[42] P. Gimeno, R. Marcé, L. Bosch, J. Comas, L. Corominas, Incorporating model uncertainty into the evaluation of interventions to reduce microcontaminant loads in rivers, Water Research 124 (2017) 415 – 424. doi:10.1016/j.watres.2017.07.036.

[43] D. Hou, X. Ge, P. Huang, G. Zhang, H. Loaiciga, A real-time, dynamic early-warning model based on uncertainty analysis and risk assessment

for sudden water pollution accidents, Environmental Science and Pollution Research 21 (2014) 8878–8892. doi:10.1007/s11356-014-2936-2.

[44] N. McIntyre, T. Wagener, H. Wheater, S. Chapra, Risk-based modelling of surface water quality: A case study of the Charles River, Massachusetts, Journal of Hydrology 274 (2003) 225–247. doi:10.1016/S0022-1694(02)00417-1.

[45] R. Bahadur, W. Samuels, Modeling the fate and transport of a chemical spill in the Elk River, West Virginia, Journal of Environmental Engineering 141 (2015) 05014007. doi:10.1061/(ASCE)EE.1943-7870.0000930.

[46] T. J. Cox, D. F. Turner, G. J. Pelletier, A. Navato, Stochastic water quality modeling of an impaired river impacted by climate change, Journal of Environmental Engineering 141 (2015) 04015035. doi:10.1061/(ASCE)EE.1943-7870.0000971.

[47] S. Rehana, P. Mujumdar, Climate change induced risk in water quality control problems, Journal of Hydrology 444-445 (2012) 63 – 77. doi:10.1016/j.jhydrol.2012.03.042.

[48] E. Ani, M. Hutchins, A. Kraslawski, P. Agachi, Assessment of pollutant transport and river water quality using mathematical models, Revue Roumaine De Chimie 55 (2010) 285.

[49] F. Benkhaldoun, I. Elmahi, M. Seaid, Well-balanced finite volume schemes for pollutant transport by shallow water equations on unstructured meshes, Journal of Computational Physics 226 (2007) 203. doi:10.1016/j.jcp.2007.04.005.

[50] K. Kachiashvili, D. Gordeziani, R. Lazarov, D. Melikdzhanian, Modeling and simulation of pollutants transport in rivers, Applied Mathematical Modelling 31 (2007) 1371–1396. doi:10.1016/j.apm.2006.02.015.

[51] P. A. Ray, L. Bonzanigo, S. Wi, Y.-C. E. Yang, P. Karki, L. E. García, D. J. Rodriguez, C. M. Brown, Multidimensional stress test for hydropower investments facing climate, geophysical and financial uncertainty, Global Environmental Change 48 (2018) 168–181. doi:10.1016/j.gloenvcha.2017.11.013.

[52] P. A. Ray, M. d. Taner, K. E. Schlef, S. Wi, H. F. Khan, S. S. G. Freeman, C. M. Brown, Growth of the decision tree: Advances in bottom-up climate change risk management, JAWRA Journal of the American Water Resources Association 55 (2019) 920–937. doi:10.1111/1752-1688.12701.

[53] M. Gharamti, B. Ait-El-Fquih, I. Hoteit, An iterative ensemble kalman filter with one-step-ahead smoothing for state-parameters estimation of contaminant transport models, Journal of Hydrology 527 (2015) 442 – 457. doi:10.1016/j.jhydrol.2015.05.004.

[54] D. M. Di Toro, J. J. Fitzpatrick, R. V. Thomann, Documentation for water quality analysis simulation program (WASP) and model verification program (MVP), in: Hydroscience, Inc., 1983, pp. 68–01–3872.

[55] R. B. Ambrose, T. A. Wool, Wasp8 stream transport model theory and user's guide: supplement to water quality analysis simulation program (WASP) user documentation, in: U. S. EPA Office of Research and Development, Washington, D.C., 2017, pp. 1–76.

[56] Tetra Tech Inc., Theoretical and computational aspects of sediment and contaminant transport in EFDC. A report to the U.S. Environmental Protection Agency, 2002.

[57] J. M. Hamrick, A Three-Dimensional Environmental Fluid Dynamics Computer Code : Theoretical and computational aspects. Special report in applied marine science and ocean engineering; special report 317, Technical Report, The College of William and Mary, Virginia Institute of Marine Science, 1992.

[58] Z. Cao, C. Xia, G. Pender, Q. Liu, Shallow water hydro-sediment-morphodynamic equations for fluvial processes, Journal of Hydraulic Engineering 143 (2017) 02517001. doi:10.1061/(ASCE)HY.1943-7900.0001281.

[59] P. Hu, Z. Cao, G. Pender, G. Tan, Numerical modelling of turbidity currents in the Xiaolangdi reservoir, Yellow River, China, Journal of Hydrology 464-465 (2012) 41 – 53. doi:10.1016/j.jhydrol.2012.06.032.

[60] Z. He, L. Zhao, P. Hu, C. Yu, Y.-T. Lin, Investigations of dynamic behaviors of lock-exchange turbidity currents down a slope based on direct numerical simulation, Advances in Water Resources 119 (2018) 164 – 177. doi:10.1016/j.advwatres.2018.07.008.

[61] X. Liu, A. Beljadid, A coupled numerical model for water flow, sediment transport and bed erosion, Computers & Fluids 154 (2017) 273 – 284. doi:10.1016/j.compfluid.2017.06.013, iCCFD8.

[62] P. Hu, Y. Lei, J. Han, Z. Cao, H. Liu, Z. He, Z. Yue, Improved local time step for 2d shallow-water modeling based on unstructured grids, Journal of Hydraulic Engineering 145 (2019) 06019017. doi:10.1061/(ASCE)HY.1943-7900.0001642.

[63] M. d. Taner, P. Ray, C. Brown, Incorporating multidimensional probabilistic information into robustness-based water systems planning, Water Resources Research 55 (2019) 3659–3679. doi:10.1029/2018WR022909.

[64] T. B. Wild, D. P. Loucks, Managing flow, sediment, and hydropower regimes in the sre pok, se san, and se kong rivers of the Mekong basin, Water Resources Research 50 (2014) 5141–5157. doi:10.1002/2014WR015457.

[65] C. Brown, Y. Ghile, M. Laverty, K. Li, Decision scaling: Linking bottom-up vulnerability analysis with climate projections in the water sector, Water Resources Research 48 (2012). doi:10.1029/2011WR011212.

[66] F. Behzadi, B. Shamsaei, J. Newman, Solution of fully-coupled shallow water equations and contaminant transport using a primitive-variable Riemann method, Environmental Fluid Mechanics 18 (2018) 515–535. doi:10.1007/s10652-017-9571-7.

[67] F. Behzadi, P. A. Ray, A Computational Fluid Dynamics Modeling Approach to Water Quality Risk Assessment: Case Study of Cincinnati, Ohio, in: AGU Fall Meeting Abstracts, volume 2018, 2018, pp. H22E–07.

[68] A. Whelton, L. McMillan, C. Novy, K. White, X. Huang, Case study: The crude mchm chemical spill investigation and recovery in west virginia usa, Environmental Science-Water Research & Technology 3 (2017) 312–332. doi:10.1039/c5ew00294j.

[69] W. M. Grayman, R. A. Deininger, R. M. Males, Design of Early Warning and Predictive Source-water Monitoring Systems, AWWA Research Foundation and American Water Works Association, Cincinnati, Ohio 45208, 2001.

[70] G. W. Brunner, Performing a water quality analysis, in: HEC-RAS River Analysis System User's manual, Version 5.0, US Army Corps of Engineers, Institute for Water Resources, Hydrologic Engineering Center (HEC), Davis, CA., 2016, pp. 19–1–19–69.

[71] WASP, Water quality analysis simulation program, https://www.epa.gov/ceam/water-quality-analysis-simulation-program-wasp, 2019.

[72] United States Environmental Protection Agency, Environmental fluid dynamics code (EFDC), https://www.epa.gov/ceam/environmental-fluid-dynamics-code-efdc, 2007.

[73] F. Behzadi, C. D. Wallace, D. Ward, H. Zhou, R. Versteeg, M. R. Soltanian, Bed form-induced hyporheic exchange and geochemical hotspots, Advances in Water Resources 156 (2021) 104025. doi:https://doi.org/10.1016/j.advwatres.2021.104025.

[74] E. F. Toro, Riemann Solvers and Numerical Methods for Fluid Dynamics, A Practical Introduction., Springer, Berlin, Heidelberg, 2009.

[75] F. Behzadi, J. C. Newman, An exact source-term balancing scheme on the finite element solution of shallow water equations, Computer Methods in Applied Mechanics and Engineering 359 (2020) 112662. doi:10.1016/j.cma.2019.112662.

[76] F. Behzadi, Solution of fully-coupled shallow water equations and contaminant transport using a primitive variable Riemann solver and a semi-discrete SUPG method, Ph.D. thesis, The University of Tennessee at Chattanooga, 2016.

[77] E. Toro, Riemann problems and the WAF method for solving the 2-dimensional shallow-water equations, Philosophical Transactions of the Royal Society A-Mathematical Physical and Engineering Sciences 338 (1992) 43–68. doi:10.1098/rsta.1992.0002.

[78] T. Weiyan, Shallow Water Hydrodynamics: Mathematical Theory and Numerical Solution for a Two-dimensional System of Shallow Water Equations, Elsevier Science Publishing Company, New York, 1992.

[79] D. Zhao, H. Shen, J. Lai, G. Tabios, Approximate riemann solvers in fvm for 2d hydraulic shock wave modeling, Journal of Hydraulic Engineering-Asce 122 (1996) 692–702. doi:10.1061/(ASCE)0733-9429(1996)122:12(692.

[80] J. E. Dennis, R. B. Schnabel, Numerical Methods for Unconstrained Optimization and Nonlinear Equations, Society for Industrial and Applied Mathematics, 1996. doi:10.1137/1.9781611971200.

[81] Y. Saad, Iterative Methods for Sparse Linear Systems, second ed., Society for Industrial and Applied Mathematics, 2003. doi:10.1137/1.9780898718003.

[82] R. Drum, J. Noel, J. Kovatch, L. Yeghiazarian, H. Stone, J. Stark, D. Raff, Ohio River Basin-formulating climate change mitigation/adaptation strategies through regional collaboration with the ORB alliance., Technical Report, U.S. Army Corps of Engineers and Ohio River Basin Alliance, Institute for Water Resources, Responses to Climate Change Program, 2017.

[83] United States Environmental Protection Agency, Toxic chemical release inventory reporting forms and instructions; revised 2016 version, Section 313 of The Emergency Planning and Community Right-to-Know Act (Title III of the Superfund Amendments and Re-authorization Act of 1986), 2016.

[84] ORSANCO, Ohio River Valley Water Sanitation Commission Annual Report, 2017.

[85] R. Herrick, J. Buckholz, F. Biro, A. Calafat, X. Ye, C. Xie, S. Pinney, Polyfluoroalkyl substance exposure in the Mid-Ohio River Valley, 1991-

2012, Environmental Pollution 228 (2017) 50–60. doi:10.1016/j.envpol.2017.04.092.

[86] U. G. C. R. P. United States Environmental Protection Agency, What climate change means for Ohio, 2016.

[87] Z. Zhu, A. Wasti, T. Schade, P. A. Ray, Techniques to evaluate the modifier process of National Weather Service flood forecasts, Journal of Hydrology X 11 (2021) 100073. doi:10.1016/j.hydroa.2020.100073.

[88] T. Adams, S. Chen, R. Davis, T. Schade, D. Lee, The Ohio River Community HEC-RAS Model, 2010, pp. 1512–1523. doi:10.1061/41114(371)160.

[89] B. Whitteberry, Ohio river pollution control standards changing; Ohio, Kentucky to use federal guidelines, Local12 (2019). URL: https://local12.com/news/local/ohio-river-pollution-control-standards-changing-ohio-ky-to-use-federal-guidelines.

[90] United States Environmental Protection Agency, U.S. Environmental Protection Agency Pollution/Situation Report: Duke Energy Cincinnati Diesel Spill-Removal Polrep., 2014.

[91] United States Environmental Protection Agency, Benchmark River Barge Spill, 2017.

[92] E. E. Yard, M. W. Murphy, C. Schneeberger, J. Narayanan, E. Hoo, A. Freiman, L. S. Lewis, V. R. Hill, Microbial and chemical contamination during and after flooding in the Ohio River—Kentucky, 2011, Journal of Environmental Science and Health, Part A 49 (2014) 1236–1243. doi:10.1080/10934529.2014.910036.

[93] U.S. Geological Survey, Surface Water for USA: Streamflow Measurements, https://waterdata.usgs.gov/nwis/measurements?, 2018.

[94] G. L. Squires, Practical Physics, 4 ed., Cambridge University Press, 2001. doi:10.1017/CBO9781139164498.

[95] L. Stolze, F. Volpin, Modeling of the Elk River spill 2014, Environmental Science and Pollution Research 22 (2015) 7980–7985. doi:10.1007/s11356-015-4331-z.

[96] R. Thomann, J. Mueller, Principles of Surface Water Quality Modeling and Control, 1987.

[97] Personal communication with Bruce Whitteberry, MCHM concentration level from Greater Cincinnati Water Works sampling, Cincinnati, Ohio, USA., 2018.

[98] H. B. Fischer, E. J. List, R. C. Koh, J. Imberger, N. H. Brooks, Mixing in Inland and Coastal Waters, Academic Press, San Diego, 1979.

[99] National Weather Service, Advanced Hydrologic Prediction Service, https://water.weather.gov/ahps2/hydrograph.php?wfo=iln\&gage=ccno1, 2018.

[100] Ohio River Valley Water Sanitation Commission (ORSANCO), Ohio River Navigational Dams, http://www.orsanco.org/river-facts/navigational-dams/ohio-river-navigational-dams/, 2021.

[101] West Virginia Testing Assessment Project (WVTAP), Appendix M: West Virginia Testing Assessment Project (WV TAP) Literature Review, v1.6, 2014.

[102] C. Brown, S. Steinschneider, P. Ray, S. Wi, L. Basdekas, D. Yates, Decision Scaling (DS): Decision Support for Climate Change, Springer International Publishing, Cham, 2019, pp. 255–287. URL: 10.1007/978-3-030-05252-2_12. doi:10.1007/978-3-030-05252-2_12.

[103] S. Steinschneider, P. Ray, S. H. Rahat, J. Kucharski, A Weather-Regime-Based Stochastic Weather Generator for Climate Vulnerability Assessments of Water Systems in the Western United States, Water Resources Research 55 (2019) 6923–6945. doi:10.1029/2018WR024446.

- RANK allows for variable channel width, water depth, and velocity leading to accurate results.
- RANK considers uncertainty of climate, pollution source, and infrastructure operations.
- RANK is tuned for stress testing on water contamination and water supply interruption.
- RANK is suited for climate change risk assessments to evaluate the water quality impacts.

Declaration of interests

☐The authors declare that they have no known competing financial interests or personal relationships that could have appeared to influence the work reported in this paper.

☒The authors declare the following financial interests/personal relationships which may be considered as potential competing interests:

Faranak Behzadi reports financial support was provided by Ohio Water Resources Center.